Random fluctuations of the firing rate function in a continuum neural field model

C. A. Brackley and M. S. Turner
Department of Physics, University of Warwick, Coventry CV4 7AL, United Kingdom
(Received 15 August 2006; revised manuscript received 16 January 2007; published 25 April 2007)

We incorporate a source of noise into a continuum neural field model by allowing the firing threshold to fluctuate noisily about a mean value, and examine traveling wave front solutions. Under certain conditions we are able to calculate the first and second moments of the distributions of the resulting time varying front speed and shape. This is then compared with more complete numerical solutions. Fluctuations in the wave front speed and in the shape (i.e., fluctuations in activity at particular coordinate positions across the wave front) were found to increase as the magnitude of the fluctuations in firing threshold increased. The mean speed was found to *increase* as the magnitude of the fluctuations increases. The role of the correlation time for the threshold variation is also investigated. We also study the role of threshold fluctuations in the failure of front propagation, both in the fast and slow varying noise limits.

DOI: 10.1103/PhysRevE.75.041913 PACS number(s): 87.19.La, 87.10.+e, 87.18.Sn

I. INTRODUCTION

A popular approach to modeling large scale neural systems developed over several years is the so-called continuum neural field (CNF) model. First developed by authors such as Amari [1] and Wilson and Cowan [2], these treat neural tissue not as an array of discrete cells, but as a continuum of neurons, with each point in space characterized by the average membrane potential, or "activity" of cells at that point. Another key idea common to these models is that the action potential mechanism which facilitates intercellular communication can be described in a very simple way, where the rate of production of action potentials of a cell is a simple function of its activity (the firing rate function). This is found experimentally to approximate a nonlinear sigmoid function as a result of the sum over the different thresholds of many neurons.

An excellent recent review of CNF models [3] discusses the many kinds of solutions and highlights their importance and relevance to real systems. For example, a great deal of work has been done on stationary and traveling wave fronts and pulses [4–6], which are thought to be of importance in applications such as models of memory [7] and understanding certain pathologies, such as epilepsy [8].

The aim of this paper is to address the role of "noisy" variation in the firing rate function. The true mechanism of action potential generation is complex, and depends on the opening, closing, and deactivation of several kinds of ion channel on the neuronal membrane. Such dynamics depends on factors such as previous stimulus and the presence of certain chemicals which can vary over long time scales. Thus the firing is ultimately a stochastic process. Single cells have been modeled extensively using several methods, for example, the stochastic Fitzhugh-Nagumo neurons studied by Tuckwell and Rodriguez [9]. However, these types of model are impractical for looking at the large numbers of neurons present in the systems modeled by CNF theories, so the identification of an extension to the CNF model, which includes such ideas, is our motivation here.

The many recovery and feedback processes, which act to reduce the firing rate of a cell after prolonged stimulation, have already been successfully included in CNF models in the form of negative feedback (or recovery). Here we instead focus on the role of a "noisy" time varying mechanism for action potential generation. If one assumes that there is coherence between fluctuation in the firing threshold of cells in the same local environment, then at the continuum level one would expect to see a firing rate function that fluctuates in time and space, and that these fluctuations might be correlated at some length scale. It is known that neurons communicate using local chemical signals although there is no direct experimental data for the spatial correlation length of the firing threshold. In what follows we will adopt the simplest possible approach in which the firing threshold, while fluctuating in value, is assumed to be uniform in the region of neural tissue of interest. Reassuringly, our results for the velocity variation and shape of the wave front in one dimension only require that the threshold be correlated on the spatial scale of the width of the wave front, itself a few times the typical intercellular connection distance. Thus our model could be directly applied to the propagation of neural activity along thin neural "channels" of highly interconnected neurons such as are found in, e.g., the infrapyramidal bundle. Additionally, we see this model as being informative in the same spirit as similar, rather crude, approximations for, e.g., the homogeneity and isotropy of the function describing spatial connectivity between cells [2]. These models have been of enduring interest in the literature and have stimulated interest in the role of varying cellular connectivity. Surprisingly, until now, there have been no studies on the role of temporal fluctuations in the firing threshold.

As a starting point we incorporate a fluctuating firing threshold into the simplest continuum model with no feedback or recovery. Section II describes the standard CNF model used, while Sec. III details the extension of this to include noise. Small fluctuations allow a perturbative approach to be used; the effect on traveling front solutions is examined first analytically, and then numerically in Sec. IV. In Sec. V we look at what happens should the threshold move into a range of values where solutions become unstable, and Sec. VI discusses the implications of the findings, suggesting further work which could include "noisy" firing functions in more realistic models.

II. MODEL

Many one-dimensional continuum models [1–3] describe the activity of cells $u(x,t)$ using the equation

$$\tau\frac{\partial u(x,t)}{\partial t} + u(x,t) = \int_{-\infty}^{\infty} w(|x-x'|)f(u(x',t))dx', \qquad (1)$$

where $w(|x-x'|)$ is the weight function for connections from cells at position x' to cells at x, and it is assumed that the activity of cells at x depends on some function f of the activity of afferent cells. The constant τ is the synaptic response time, and gives the characteristic time of a neuron's response to an instantaneous input. Other assumptions are that the connection strength depends only on distance to afferent cells (i.e., the system is homogeneous), and that propagation times for action potentials are negligible.

Much previous work has involved so-called "Mexican hat" connection functions (for example, a difference of Gaussians), which correspond physically to local excitatory (positive) connections and long range inhibitory (negative) connections. These yield several interesting solutions. As in other work [4–6], the Heaviside step function is used as a first approximation to the firing rate function as it allows some progress to be made analytically. In this and the following sections we use

$$f(u) = \Theta(u-\theta), \qquad (2)$$

$$w(|y|) = \left(1 - \frac{|y|}{2\alpha}\right)e^{-|y|/\alpha}, \qquad (3)$$

where θ is the firing threshold. For convenience w is normalized to unity, $\int_{-\infty}^{\infty} w(x)dx = 1$, and $\tau = \alpha = 1$ throughout, which corresponds to a choice of units for time (τ) and space (α), respectively.

The types of solution of interest to us here are primarily traveling wave fronts. It has been shown [10] that when the system is arranged so that there are three steady states $\bar{u}_1 < \bar{u}_2 < \bar{u}_3$, there exist traveling front solutions where the wave connects the stable steady states [i.e., $u(-\infty,t) = \bar{u}_3$ and $u(\infty,t) = \bar{u}_1$]. By setting $\partial_t u(x,t) = 0$ and $u(x,t) = \bar{u}$ in Eq. (1), the steady states are solutions of $\bar{u} = \kappa f(\bar{u})$, where $\kappa = \int_{-\infty}^{\infty} w(y)dy = 1$; i.e., $\bar{u}_1 = 0$, $\bar{u}_2 = \theta$, and $\bar{u}_3 = 1$. Following [3], the shape of this front can be found by changing to coordinates where the front is stationary and using Green's function methods to convert the equation to a purely integral form

$$U(\xi,t) = \int_0^{\infty} \eta(s)\int_{-\infty}^{\infty} w(y)f(U(\xi - y + cs, t-s))dyds, \qquad (4)$$

where $\xi = x - ct$ with c the speed of the front, $y = x - x'$, and $\eta(s)$ the Green's function for the operator $(1+\partial_t)$ where

$$\eta(s) = \begin{cases} e^{-s}, & s \geq 0 \\ 0, & s < 0. \end{cases} \qquad (5)$$

Wave front solutions are those where $U(\xi,t) = q(\xi)$ with

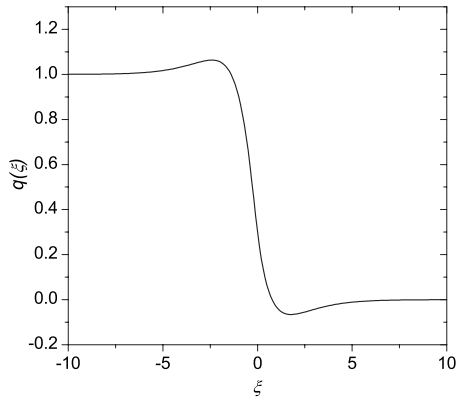

FIG. 1. Plot showing wave front activity q as a function of position ξ (in moving coordinates where the front is stationary) when $\theta = 0.3$. The front connects the two stable steady states $\bar{u}_3 = 1$ and $\bar{u}_1 = 0$. In the lab frame (x) the front would be moving to the right.

$$q(\xi) = \int_0^{\infty} ds \int_{-\infty}^{\infty} dy\, \eta(s)w(y)f(q(\xi - y + cs)), \qquad (6)$$

from which an equation for the speed c can be found by choosing the origin of the coordinates $q(0) = \theta$. A plot of the activity (wave) front with $\theta = 0.3$ is shown in Fig. 1. As a function of threshold the speed of the front c is given by

$$c = \begin{cases} -1 + \dfrac{1}{\sqrt{2\theta}}, & 0 < \theta \leqslant 0.5 \\ 1 - \dfrac{1}{\sqrt{2(1-\theta)}}, & 0.5 < \theta < 1. \end{cases} \qquad (7)$$

Note the symmetry about the point $\theta = 0.5$, with c positive if $\theta < 0.5$ (an advancing front), and negative if $\theta > 0.5$ (a receding front).

The linear stability can be obtained by expanding $U(\xi,t) = q(\xi) + \delta u(\xi)e^{\lambda t}$ in Eq. (4). This gives an eigenvalue equation $u = \mathcal{L}u$ of the form

$$u(\xi) = \int_0^{\infty} \eta(s)\int_{-\infty}^{\infty} w(y)f'(q(\xi - y + cs))u(\xi - y + cs) \times e^{-\lambda s}dyds. \qquad (8)$$

The solution is stable if $\mathrm{Re}[\lambda] < 0$ for $\lambda \neq 0$; the eigenvalues λ, can be found as in [3,11] using the Evan's function method, which gives

$$\lambda(\theta) = \begin{cases} \dfrac{-2}{1+\sqrt{2\theta}}, & 0 < \theta < 0.5 \\ \dfrac{-2}{1+\sqrt{2(1-\theta)}}, & 0.5 < \theta < 1. \end{cases} \qquad (9)$$

Thus the solution is stable for all θ (note, however, the requirement that $0 < \theta < 1$ in order for there to be two steady states for the wave front to connect).

III. FLUCTUATING FIRING FUNCTIONS IN WAVE FRONT SOLUTIONS

As discussed in Sec. I we seek to study noisy variation of the firing threshold of individual neurons. At the continuum level we expect to see a firing rate function which fluctuates in time and space, and that may be correlated on some length and time scales.

A major simplification can be made since we are interested in studying traveling wave fronts. In this case the only important fluctuations in the threshold are those of neurons near the "face" of the wave front (a distance only several times the width α of the connection function). The velocity and shape of the wave front is insensitive to the threshold further from the front. By assuming that the threshold is the same across the wave front (that it is correlated on this spatial length scale) then we can treat the threshold as varying uniformly across the *entire* system.

A threshold, which varies randomly about a mean value, can be written as

$$\theta(t) = \bar{\theta} + \delta\theta(t), \tag{10}$$

where $\bar{\theta}$ is the mean value of $\theta(t)$ and $\delta\theta(t)$ is taken to have the physical analogue of the displacement of a particle subject to random forces (in a one-dimensional harmonic potential). Here we take

$$\delta\theta(t) = \int_0^t e^{-(t-t')/\nu} h(t')dt', \tag{11}$$

in which ν is a characteristic time constant for this variation, e.g., appearing in the correlation function $\langle \delta\theta(0)\delta\theta(t)\rangle$. The noise term $h(t)$ is chosen to be a Gaussian random variable defined by $\langle h(t)\rangle = 0$ and $\langle h(t)h(t')\rangle = a\delta(t-t')$ (where angular brackets denote the average over realizations of the system), meaning

$$\langle \delta\theta(t)\rangle = 0, \tag{12}$$

$$\langle \delta\theta(0)\delta\theta(t)\rangle = \frac{a\nu}{2} e^{-|t|/\nu}. \tag{13}$$

The fluctuations are described by two variables: an amplitude $a\nu/2$ and a time ν. Choosing large ν and small a gives a small slowly varying fluctuation in the firing threshold about a mean value $\bar{\theta}$.

A. Effect on the shape of the wave front

As described in Sec. II for step function f the shape of the front $q(\xi)$ can be found explicitly for a particular choice of θ. The system is still translationally invariant, and we now use the coordinate system where $\xi = x - c(t)t$ with the point $\xi = 0$ where $q = \theta(t)$. At any instant in time there is a solution $q(\xi, \theta(t))$, however, as the activity is found by integrating over all previous times the actual shape $U(\xi,t)$ will differ from this. At any instant one can therefore expect a decay away from the instantaneous shape towards $q(\xi, \theta(t))$,

$$\frac{\partial U(\xi,t)}{\partial t} = \lambda(\theta(t))[U(\xi,t) - q(\xi,\theta(t))], \tag{14}$$

where λ is a Lyapunov constant and is also assumed to depend on $\theta(t)$. Integrating this gives

$$U(\xi,t) = U(\xi,0)e^{\lambda(\theta)t} - \int_0^t e^{-\lambda(\theta)(t'-t)}\lambda(\theta)q(\xi,\theta)dt'. \tag{15}$$

If it is assumed that $\theta(t)$ is sufficiently slowly varying with t, then this simplifies to

$$U(\xi,t) \approx q(\xi,\theta) + [U(\xi,0) - q(\xi,\theta)]e^{\lambda(\theta)t}. \tag{16}$$

Writing $\delta u(\xi,\theta) = [U(\xi,0) - q(\xi,\theta)]$, and inserting this into Eq. (4) gives an eigenvalue equation $\delta u = \mathcal{L}\delta u$, with $\mathcal{L}$ the same operator as in Eq. (8) with eigenvalue $\lambda(\theta)$ as given in Eq. (9). The fact that $\lambda(\theta)$ is negative for all θ means $U(\xi,t)$ will always decay towards $q(\xi,\theta(t))$, and the solution remains stable.

Returning to Eq. (14) and using Eq. (10), $q(\xi,\theta(t))$ and $\lambda(\theta)$ can be expanded about $\bar{\theta}$ giving

$$\frac{\partial U(\xi,t)}{\partial t} = \left(\lambda_{\bar{\theta}} + \delta\theta(t) \left.\frac{\partial\lambda}{\partial\theta}\right|_{\bar{\theta}}\right)[U(\xi,t) - q_{\bar{\theta}}(\xi) - \delta\theta(t)g(\xi)], \tag{17}$$

where $\lambda_{\bar{\theta}} = \lambda(\bar{\theta})$, $q_{\bar{\theta}}(\xi) = q(\xi,\bar{\theta})$, and $g(\xi) = \partial_\theta q(\xi,\bar{\theta})$.

Defining $\Delta U(\xi,t) = U(\xi,t) - q_{\bar{\theta}}(\xi)$ allows this to be rewritten as

$$\frac{\partial \Delta U(\xi,t)}{\partial t} = \lambda_{\bar{\theta}}[\Delta U(\xi,t) - \delta\theta(t)g(\xi)], \tag{18}$$

where it has been assumed that ΔU and $\delta\theta(t)$ are small, so terms in $\delta\theta(t)^2$ and $\delta\theta(t)\Delta U(\xi,t)$ are to be neglected. This can be integrated and the mean and mean squared variations calculated. In the long time limit these approach

$$\langle \Delta U(\xi,t)\rangle = 0, \tag{19}$$

$$\langle \Delta U(\xi,t)^2\rangle = \frac{a\nu}{2}\frac{\lambda_{\bar{\theta}}^2 g(\xi)^2}{(\lambda_{\bar{\theta}}^2 - 1/\nu^2)}. \tag{20}$$

Using the definition of ΔU, and $\langle \delta\theta(t)^2\rangle = a\nu/2$, the first and second moments of $U(\xi,t)$ are

$$\langle U(\xi,t)\rangle = q_{\bar{\theta}}(\xi), \tag{21}$$

$$\langle (U(\xi,t) - \langle U(\xi,t)\rangle)^2\rangle = \langle \delta\theta(t)^2\rangle \frac{\lambda_{\bar{\theta}}^2 g(\xi)^2}{(\lambda_{\bar{\theta}}^2 - 1/\nu^2)}. \tag{22}$$

Thus, as one might expect, the magnitude of the fluctuations in the shape of the wave are proportional to both the magnitude of the firing threshold fluctuations, and the rate of change of q with respect to threshold, which is itself a function of position.

B. Effect on the speed of the wave front

In Sec. II the speed of the front c is found as a function of θ by using $q(0)=\theta$ in Eq. (6), giving Eq. (7). With time varying threshold, by assuming that $\delta\theta(t)$ is small we can use $q(0)=\theta(t)$, and expand $\theta(t)=\bar{\theta}+\delta\theta(t)$ in Eq. (7) giving

$$c(t) = -1 + \frac{1}{\sqrt{2\bar{\theta}}}\left(1 - \frac{\delta\theta(t)}{2\bar{\theta}} + \frac{3\delta\theta(t)^2}{8\bar{\theta}^2} - \frac{5\delta\theta(t)^3}{16\bar{\theta}^3} + \frac{35\delta\theta(t)^4}{128\bar{\theta}^4}\right), \tag{23}$$

keeping terms up to fourth order. Noting the symmetry about $\theta=0.5$, here (and in the rest of this section) we quote only the results for the $0<\theta<0.5$ case for clarity. The mean and variance of the distribution of speeds can then easily be found to be

$$\langle c(t)\rangle = -1 + \frac{1}{\sqrt{2\bar{\theta}}}\left(1 + \frac{3\langle\delta\theta(t)^2\rangle}{8\bar{\theta}^2} + \frac{105\langle\delta\theta(t)^2\rangle^2}{128\bar{\theta}^4}\right), \tag{24}$$

$$\langle(c(t) - \langle c(t)\rangle)^2\rangle = \frac{\langle\delta\theta(t)^2\rangle}{8\bar{\theta}^3} + \frac{39\langle\delta\theta(t)^2\rangle^2}{64\bar{\theta}^5} + \frac{1005\langle\delta\theta(t)^2\rangle^3}{512\bar{\theta}^7}. \tag{25}$$

For the purposes of comparison with our later numerical calculations, it is necessary to include terms in powers of $\langle\delta\theta(t)^2\rangle$ up to 2 in the mean and 3 in the variance due to the high powers of $\bar{\theta}$ in the denominator of these terms.

As expected, as the magnitude of the fluctuations (measured by $\langle\delta\theta(t)^2\rangle$) increase, so too does the magnitude of the fluctuations in the speed. An unforeseen result is that the mean front speed *increases* with increasing fluctuations in firing threshold (at least in the small $\langle\delta\theta(t)^2\rangle$ regime). This result can be traced to the shape of the $c(\theta)$ curve; as a convex function (in the interval [0,05]) it follows from Jensen's inequality that $\langle c(\theta)\rangle \geqslant c(\bar{\theta})$, so introducing fluctuations in θ will increase the mean speed.

Note that above we have assumed that there remain two stable steady states $(u=0,1)$ for the wave front to connect. In the event that θ moves outside the interval (0,1) then one of the steady states is lost, and the wave front will "die" in favor of the one remaining steady state. We reserve discussion of such an event until Sec. V.

IV. NUMERICAL SOLUTIONS

In order to test the analytical results of Sec. III and extend the study into the nonperturbative regime (establishing where the perturbative results break down), Eq. (1) was solved numerically with step function $f(u)=\Theta(u-\theta(t))$. Details of the numerical approach are given in the Appendix. In this section we again look only at the case where the wave front is stable, and thus constrain the range of values of $\langle\delta\theta(t)^2\rangle$ such that $\theta(t)$ remains in the interval $(0,1)$ within the time scales investigated.

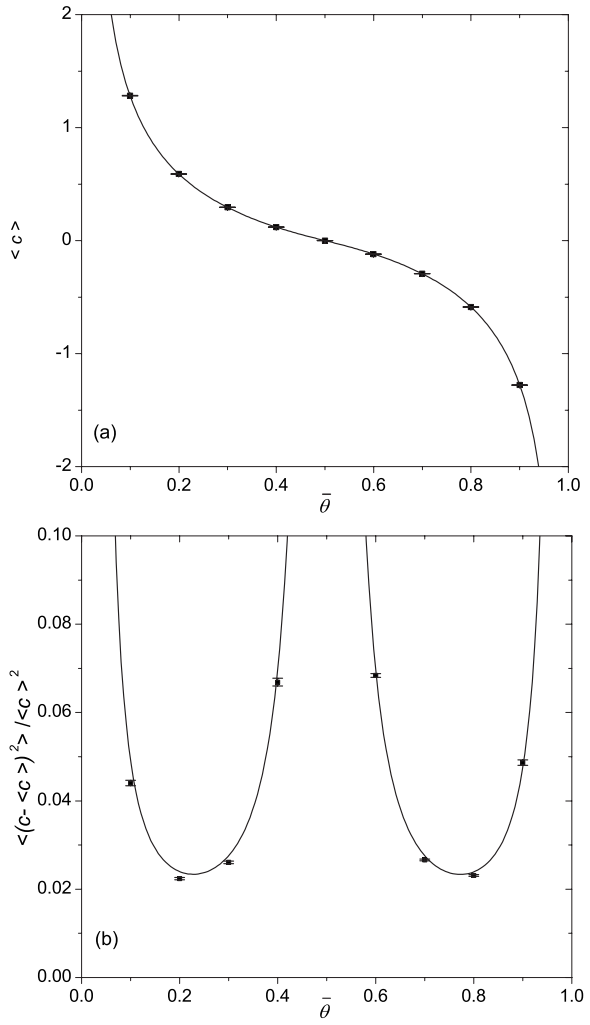

FIG. 2. Plots showing how the mean threshold $\bar{\theta}$ effects (a) the mean speed $\langle c\rangle$, and (b) the variance of the speed $\langle(c-\langle c\rangle)^2\rangle$ (normalized by $\langle c\rangle^2$). Solid lines show analytical results from Eqs. (24) and (25), and points are numerical results. The other parameters were here taken to be $\nu=20$ and $\langle\delta\theta(t)^2\rangle=5\times10^{-4}$. Error bars in this and subsequent plots are estimates of the standard deviation in the mean and variance of distributions, calculated as described in [12].

Firstly, the effect of the noise at different mean thresholds was investigated by examining the statistics of the speed of the front at different mean threshold $\bar{\theta}$ with correlation time $\nu=20$ and $\langle\delta\theta(t)^2\rangle=5\times10^{-4}$ (which is well within the region where the analytical theory is valid as shown below). It is reassuring that the mean and variance of the speed were both found to agree well with analytical perturbative results for all $0<\bar{\theta}<1$, as shown in Fig. 2. Figure 3 shows how the variance of the fluctuations in the wave front $U(\xi,t)$ vary with position for several mean firing thresholds $\bar{\theta}$. These, and similar results for other $\bar{\theta}$, exemplify the excellent agreement between the analytic perturbation theory and numerical results for all ξ.

The effect of the magnitude of the fluctuations (measured by $\langle\delta\theta(t)^2\rangle$) was investigated with a view to identifying the

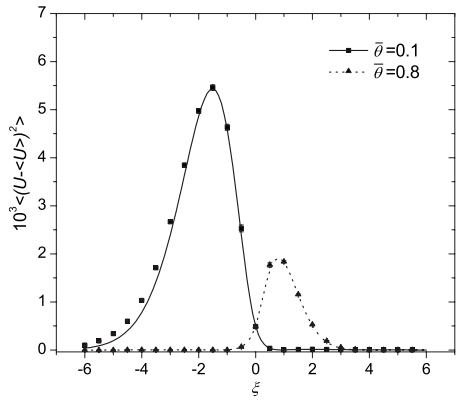

FIG. 3. Plot showing the variance of the fluctuations in $U(\xi,t)$ as a function of ξ for several different $\bar{\theta}$. The numerical solutions (points) fit closely to the analytical lines [from Eq. (21)]. The other parameters were here taken to be $\nu=20$ and $\langle\delta\theta(t)^2\rangle=5\times10^{-4}$. Where error bars are not shown they are smaller than the points.

range in which the perturbative results hold. Figure 4 shows how the mean wave speed and the variance of that speed varies with the noise in the firing threshold. In both cases the perturbative and numerical results show agreement for small fluctuations, but as expected some discrepancy appears for larger $\langle\delta\theta(t)^2\rangle$. The error in the perturbative estimate for $\langle c\rangle$, as presented in Sec. III, is found to exceed 2% for the root mean squared fluctuation amplitude of $\sqrt{\langle\delta\theta(t)^2\rangle}\geqslant0.08$. We also examined the fluctuations in $U(\xi,t)$; see Fig. 5.

Finally, the effect of varying the correlation time for the noise was investigated; i.e., ν was varied at fixed $\langle\delta\theta(t)^2\rangle$ and $\bar{\theta}$. Large correlation times ν corresponded to slowly varying noise, and $\nu\to0$ corresponds to uncorrelated noise.

Numerical results were obtained with $\bar{\theta}=0.3$ and ν varying between 0 and 35, for $\langle\delta\theta(t)^2\rangle=5\times10^{-4}$ and 5×10^{-3} (the latter corresponding to an amplitude for which the numerical results deviate from the analytical solutions; see Fig. 4). Figure 6(a) shows the effect of the time constant of the fluctuations in the firing threshold on the mean speed; when $\langle\delta\theta(t)^2\rangle$ is large the mean speed is approximately constant for ν down to order unity, after which there is a sharp decrease, which is where $\nu\to\tau=1$ (i.e., the time constant of the fluctuations approaches that of the system). In this regime one might expect that the system can no longer respond quasistatically to the fluctuations and the effects of the fluctuations therefore decrease. The perturbative theory fails, which makes numerical solutions of the sort presented here essential to the study of the small ν limit. For the small $\langle\delta\theta(t)^2\rangle$ case again there is a decrease (albeit smaller in magnitude) as $\nu\to\tau$.

For both values of $\langle\delta\theta(t)^2\rangle$ the variance of the speed decreases sharply towards zero as $\nu\to0$ [Fig. 6(b)], again consistent with the idea that the system is no longer quasistatically at "slave" to the fluctuations in the threshold as $\nu\lesssim\tau$. The small $\langle\delta\theta(t)^2\rangle$ results show that $\langle(c-\langle c\rangle)^2\rangle/\langle c^2\rangle$ converges to the asymptotic solution [from Eq. (25)] as ν gets large. In the large $\langle\delta\theta(t)^2\rangle$ results (where we do not expect the perturbation theory to apply) $\langle(c-\langle c\rangle)^2\rangle/\langle c^2\rangle$ seems to converge to some maximum value which is lower than predicted by the naive application of Eq. (25).

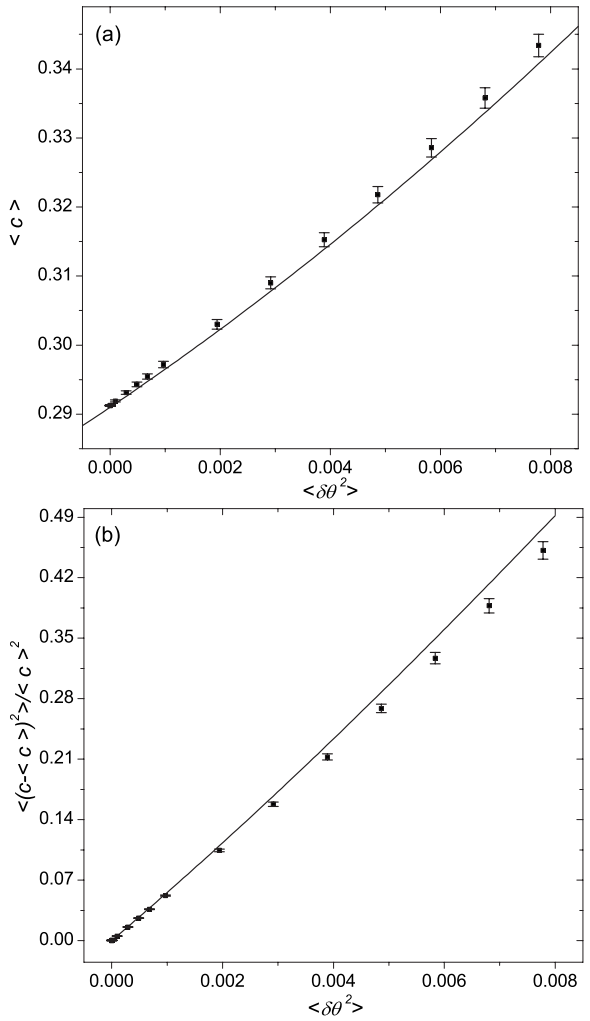

FIG. 4. Plots showing how the magnitude of the fluctuations in the firing threshold $\langle\delta\theta(t)^2\rangle$ effects (a) the mean speed, and (b) the variance of the speed (normalized by $\langle c\rangle^2$) of the front. The mean threshold and time constant of the noise were $\bar{\theta}=0.3$ and $\nu=20$, with values of $\langle\delta\theta(t)^2\rangle$ between 1×10^{-6} and 8×10^{-3}, the upper limit being set by the requirement that $\theta(t)$ remain between 0 and 1. Solid lines show analytical results from Eqs. (24) and (25), and points are numerical results. In both cases numerical results fit closely to the lines at small $\langle\delta\theta(t)^2\rangle$.

V. UNSTABLE WAVE FRONTS

We return now to the question of what happens if $\theta(t)$ should move outside the interval $(0,1)$, destroying one of the steady states. For example, should $\theta(t)$ move above one, the activity u on the left-hand side of the front (see Fig. 1) will begin to decrease exponentially towards 0. Should $\theta(t)$ move back below the now decreasing value of u, the activity will begin to increase back towards 1 and the front will survive. The wave front dies when the threshold exceeds the activity, and continues to exceed it for much of the time that the front

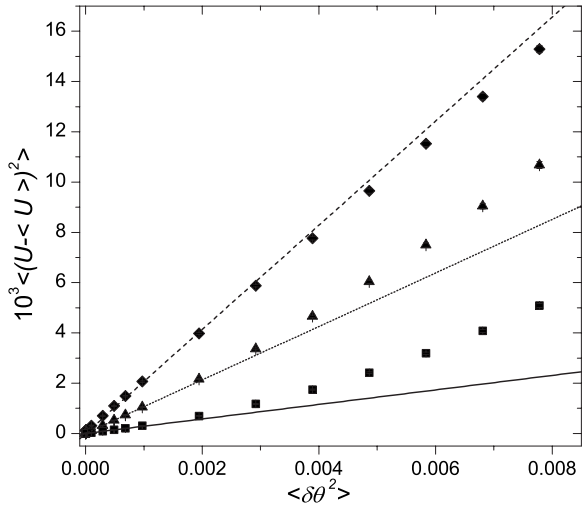

FIG. 5. Plot showing the effect on the variance in $U(\xi,t)$ of $\langle\delta\theta(t)^2\rangle$ at several values of ξ. Square, triangle, and diamond points show results for $\xi=-1.5,-1$, and -0.5, respectively, and solid, dotted, and dashed lines show theoretical relationships from Eq. (22) again for $\xi=-1.5$, -1, and -0.5, respectively. Numerical results move away from the analytical line at large $\langle\delta\theta(t)^2\rangle$. Where error bars are not shown they are smaller than the points. The values of other parameters are $\bar{\theta}=0.3$ and $\nu=20$.

subsequently takes to decay; an example of such an event is shown in Fig. 7.

It is important to understand that the introduction of noise in the firing rate function has introduced a mechanism for the destruction of a wave front that was not previously present. The dynamics of such wave front decay can be modeled by considering the activity far from the front on the left, u_L, and on the right, u_R. The initial conditions are $u_L(t=0)=1$ and $u_R(t=0)=0$ and $\theta(t=0)=\bar{\theta}$. The dynamics are governed by

$$\tau\frac{du_{L,R}}{dt}=-u_{L,R}+\Theta(u_{L,R}-\theta(t)). \tag{26}$$

We investigate this behavior numerically by examining the time for a front to decay, averaged over many realizations of the system (see the Appendix for details of the numerical work). The mean front life time t_l depends on the way in which the threshold fluctuates. In particular, it depends on how the correlation time for the fluctuations compares with the time constant τ for wave front decay. It also depends on the amplitude of the variation and on $\bar{\theta}$ (see Figs. 8 and 9).

If $\langle\delta\theta(t)^2\rangle$ is large, then $\theta(t)$ will very quickly reach 0 or 1, and is likely to spend long periods of time outside the stable range of values leading to very short lived fronts. In the case where ν is large compared to τ (very slow fluctuations) one could crudely argue that as soon as $\theta(t)$ moves outside the stable range of values the front will die before $\theta(t)$ moves back into the stable range (which is now shrinking at an exponential rate). The time t_l will therefore be dominated by the time it takes for the front to first become unstable. Again considering the analogy of $\theta(t)$ with the position of a particle in a 1D potential, this time is similar to a

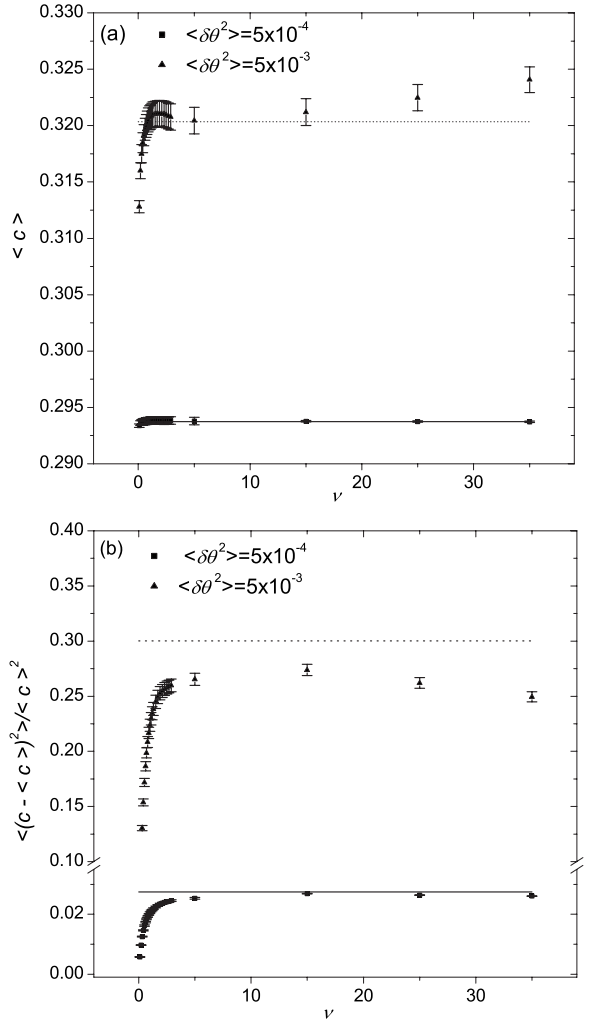

FIG. 6. Plots showing the (a) mean and (b) variance (normalized by $\langle c\rangle^2$) of the speed c for different values of ν, with $\bar{\theta}=0.3$. Solid and dotted lines show the perturbative result for large ν [from Eqs. (24) and (25)] for $\langle\delta\theta(t)^2\rangle=5\times10^{-4}$ and $\langle\delta\theta(t)^2\rangle=5\times10^{-3}$, respectively. The latter is sufficiently large that the numerical solution is diverging noticeably from the perturbation estimate. The feature that the perturbative results break down badly for $\nu\lesssim5$ is clearly visible.

"Kramer's escape time" (see [13]) so one would expect linear dependence on ν, and approximately exponential dependence on $\langle\delta\theta(t)^2\rangle$.

Our numerical work shows that the linear dependence of t_l on ν remains down to $\nu\sim\tau$, after which t_l increases with decreasing ν as shown in Fig. 8. This is because, in this fast fluctuations regime, the threshold needs to remain mostly outside the stable interval for the many correlation times ν it takes the front to decay.

Even in the small $\langle\delta\theta(t)^2\rangle$ regime there is still a finite time in which $\theta(t)$ will move outside the interval (0, 1), and as Fig. 9 shows there appears to be an approximately exponential dependence of t_l on $\langle\delta\theta(t)^2\rangle$ for $\nu\gtrsim1$. However, the dynamics are nontrivial as $\theta(t)$ may cross into and out of the range of values where the wave front is stable many times before the front is finally destroyed.

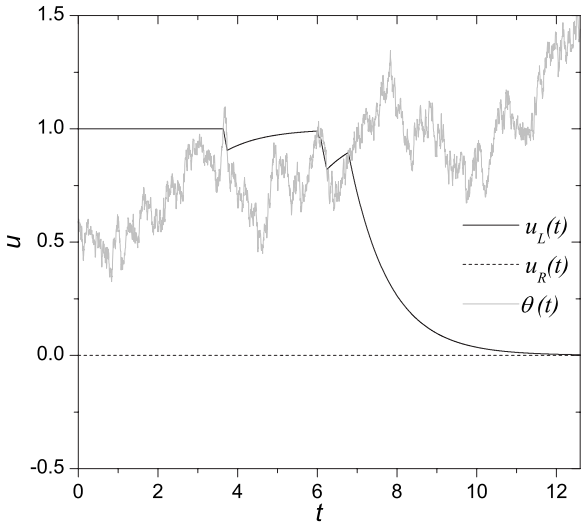

FIG. 7. Plot showing fluctuating threshold $\theta(t)$, and u_L and u_R with dynamics as given by Eq. (26). The front recovers several times before ultimately being destroyed leaving the single steady state. Here the fluctuating threshold has $\langle \delta\theta(t)^2 \rangle = 0.09$ and $\bar{\theta} = 0.7$.

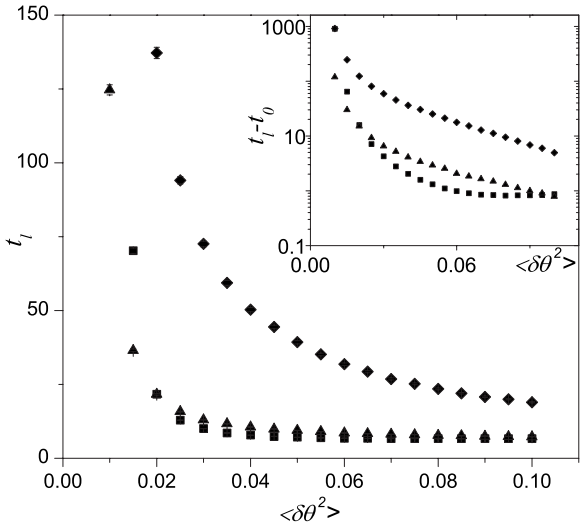

FIG. 9. Plot showing the dependence on the magnitude of threshold fluctuations of the mean wave front lifetime t_l. Other parameters are $\bar{\theta} = 0.7$. Square, triangle, and diamond points show results for $\nu = 0.1$, 1.0, and 10, respectively. The inset shows log-linear plots of $t_l - t_0$ against $\langle \delta\theta^2 \rangle$, where t_0 is an estimate of the asymptotic value of t_l. An approximately exponential relationship is seen for $\nu \gtrsim 1$ and $\langle \delta\theta^2 \rangle \gtrsim 0.03$.

VI. CONCLUSIONS

Our numerical work has shown that the results found analytically in Sec. III hold for small magnitude fluctuations up to about $\langle \delta\theta(t)^2 \rangle = 2 \times 10^{-3}$, and for slowly varying noise down to about $\nu = 5$. We have seen that if we increase $\langle \delta\theta(t)^2 \rangle$ we obtain the unforeseen result that the mean speed increases with increasing magnitude of fluctuations, with apparently no maximum, but when $\langle \delta\theta(t)^2 \rangle$ becomes large the average lifetime of a wave front drops off exponentially.

Also the correlation time of the fluctuations in the threshold has little effect on the resulting fluctuations in the speed and shape of the front, provided it is at least several times larger than τ, the time constant of the system. Also as expected, the slower the fluctuations the longer the lifetime of the front.

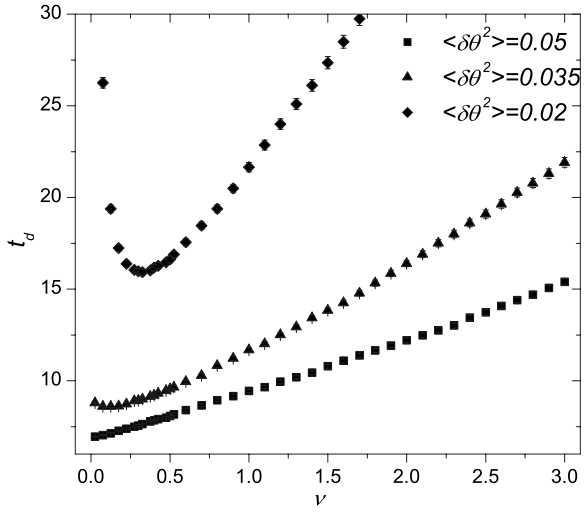

FIG. 8. Plot showing the dependence on the fluctuation correlation time ν of the mean time to wave front death t_l. This is a linear relationship with t_l decreasing with decreasing ν down to $\nu \sim \tau$; below this t_l increases with decreasing ν. This effect decreases with increasing $\langle \delta\theta(t)^2 \rangle$. Other parameters are $\bar{\theta} = 0.7$.

In the fast fluctuations (small ν) limit we find that the effects on the speed and shape of the wave front reduce as the system can no longer respond quickly enough to changes in the threshold. Also (at least in the small $\langle \delta\theta(t)^2 \rangle$ regime) the lifetime of the front begins to increase as $\nu \to 0$. These regimes are out of reach of our analytic perturbation theory.

There is much scope for further work on this problem. For example the form of the firing function could be replaced with a more realistic sigmoid function of the form

$$f(u) = \frac{1}{1 + e^{-\beta(u-\theta)}}, \tag{27}$$

in which noise could be introduced to both the threshold θ, and the steepness of the curve β. Another more realistic model would be to allow spatial variation in threshold as well as fluctuations in time. Also, more detailed models, which include feedback terms (the so-called "spike frequency adaption" models), and which exhibit other solutions, such as traveling pulses, could be examined. Here the effect of introducing noise on the stability of traveling and stationary pulses may have interesting consequences for memory models. We plan to investigate the effect of noise in similar two-dimensional models in the future.

APPENDIX: DETAILS OF NUMERICAL WORK

The numerical results of Sec. IV were obtained by solving Eq. (1) using a fourth-order Runge-Kutta routine (based on those in [14]). In order to most efficiently evaluate the con-

volution integrals a Fourier transform was performed and the product of the functions $\tilde{w}(k)$ and $\tilde{f}[u]$ calculated before inverse Fourier transforming. The transform of $w(y)$ was found analytical, while those of the step function $f(u)$ and the inverse transform were performed using a fast Fourier transform routine [15].

Spatial and temporal discretization was done with a grid size $\Delta x=0.01$ and $\Delta t=0.05$ in the units where $\tau=\alpha=1$, with all routines being written in FORTRAN 90.

The time varying threshold was generated by solving the equation

$$\frac{d\delta\theta}{dt} = -\frac{\delta\theta}{\nu} + h(t), \tag{A1}$$

using a second order stochastic Rung-Kutta routine (see [16]), with $h(t)$ as detailed in Sec. III.

Values of $u(x,t)$ were calculated over a time of 1000τ, with a system size of $L=50\alpha$ (compared to the $\sim 5\alpha$ width of the wave front feature). The position of the midpoint of the front was recorded as a function of time; this was smoothed by averaging over $8\Delta t$ at each time step, and then the derivative was found. This gives the wave front speed c as a function of time, from which the mean, second moment, and variance can be calculated. The $u(x,t)$ data was shifted to the frame of reference where the front is stationary by using an interpolation routine (from [14]) to find the point where $u(x,t)=\theta(t)$ at each time step, and setting this to be $\xi=0$; the statistics of $U(\xi,t)$ at particular ξ could then be examined.

We found in order to investigate small changes in c and u care was required to ensure that Δx and Δt were sufficiently small, in particular, when the magnitude of threshold fluctuations is very small the reliability of results has to be considered carefully. The statistical error in the mean and variance of quantities shown on plots were calculated as described in [12].

For the results of Sec. V, Eq. (26) is solved also using a fourth-order Runge-Kutta routine, with the threshold noise modeled as before. The mean time to front death was found by averaging over 5000 realizations of the system, and the error in this (shown on plots as error bars where these are larger than the points) is calculated from the sample variance [12].

[1] S. Amari, Biol. Cybern. **27**, 77 (1977).
[2] H. R. Wilson and J. D. Cowan, Cybernetics **13**, 55 (1973).
[3] S. Coombes, Biol. Cybern. **93**, 91 (2005).
[4] D. J. Pinto and G. B. Ermentrout, SIAM J. Appl. Math. **62**, 206 (2001).
[5] P. C. Bressloff, Physica D **155**, 83 (2001).
[6] S. Coombes and M. R. Owen, Phys. Rev. Lett. **94**, 148102 (2005).
[7] C. P. Fall, T. J. Lewis, and J. Rinzel, Biol. Cybern. **93**, 109 (2005).
[8] R. D. Chervin, P. A. Perice, and B. W. Conors, J. Neurophysiol. **60**, 1695 (1988).
[9] H. C. Tuckwell and R. Rodrigues, J. Comput. Neurosci. **5**, 91 (1998).
[10] G. B. Ermentrout and J. B. Mcleod, Proc. - R. Soc. Edinburgh, Sect. A: Math. **123**, 416 (1993).
[11] S. Coombes and M. R. Owen, SIAM J. Appl. Dyn. Syst. **4**, 574 (2004).
[12] G. Cowan, *Statistical Data Analysis*, 1st ed. (Oxford University Press, 1998).
[13] H. A. Kramers, Physica (Amsterdam) **7**, 284 (1940).
[14] H. Press, S. A. Teukolsky, W. T. Vetterling, and B. P. Flannery, *Numerical Recipes in Fortran*, 2nd ed. (Cambridge University Press, 1992).
[15] M. Frigo and S. G. Johnson, Proc. IEEE **93**, 216 (2005).
[16] R. L. Honeycutt, Phys. Rev. A **45**, 600 (1992).